



## Shear-type damper using a low-yield-strength circular hollow section

**Jinwoo KIM**  
Ph.D Candidate  
Osaka University  
Suita, JAPAN  
*kim\_jinwoo@arch.eng.osaka-u.ac.jp*

**Tomohiro KINOSHITA**  
Senior Researcher  
JFE STEEL Corp.  
Kanagawa, JAPAN  
*to-kinoshita@jfe-steel.co.jp*

**Susumu KUWAHARA**  
Associate Professor  
Osaka University  
Suita, JAPAN  
*kuwa@arch.eng.osaka-u.ac.jp*

**Wataru KITAMURA**  
Deputy Manager  
JFE Civil Engineering &  
Construction Corp.  
Tokyo, JAPAN  
*w-kitamura@jfe-civil.com*

**Kazuaki MIYAGAWA**  
General Manager  
JFE Civil Engineering &  
Construction Corp.  
Tokyo, JAPAN  
*miyagawa@jfe-civil.com*

### Summary

The present study investigates the mechanical behavior of a shear-type damper using a low-yield-strength circular hollow section (LYCHSD). When using a LYCHSD as a seismic energy absorbing device, the hysteresis characteristics and deformation capacity of the LYCHSD should be evaluated accurately. Thus, monotonic and cyclic loading tests were carried out on a LYCHSD, taking the aspect ratio and diameter as variable parameters. The test results were used to establish a method of calculating the full plastic shear strength and initial stiffness. In addition, it was found that the deformation capacity was inversely proportional to the aspect ratio and diameter. The monotonic loading test was also simulated using the finite element method (FEM) in order to verify the experimental results, and to evaluate the local strain around the weld toe due to the crack.

**Keywords:** Low-yield-strength circular-hollow-section damper; Aspect ratio; Diameter; Collapse mechanism; Deformation capacity; FEM analysis; Equivalent plastic strain.

### 1. Introduction

The present study attempts to reveal the hysteresis characteristics of a shear-type hysteretic damper with a low-yield-strength circular hollow section (LYCHSD). Moreover, we examine the local strain related to a crack and validate the test results by performing a finite element method (FEM) analysis of a monotonic loading test.

### 2. Loading Test Setup and Process

The specimen used in the present study is shown in detail in Fig. 1. The cross-sectional dimensions of the LYCHSD were  $\phi 130 \times 6,5$  and  $\phi 175 \times 8,8$ .  $D/t$  of the two cross-sections are approximately the same at 20,0 and 19,9, respectively. Specimens having  $h/D$  of 1,00, 1,25, and 1,50 were examined. The loading system is shown in Fig. 2. As can be seen, the specimen was fixed to the loading beam, and a horizontal force was applied at the center height of the specimen using a 200-ton jack. There were four types of loading: monotonic loading, incremental cyclic loading, 3% and 5% steady-amplitude cyclic loading.

### 3. Test result

Figure 3 shows an example of the cyclic loading results. All of the specimens under cyclic loading



Photo 1: Failure mode

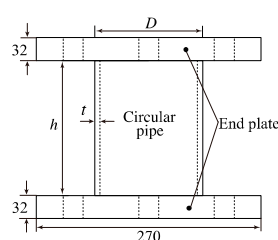


Fig. 1: Details of Specimens

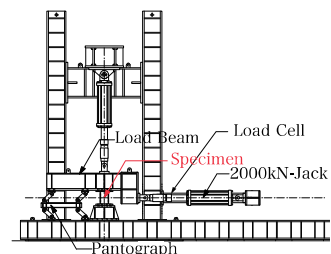


Fig. 2: Loading system

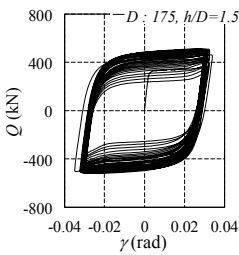


Fig. 3:  $Q-\gamma$  relation

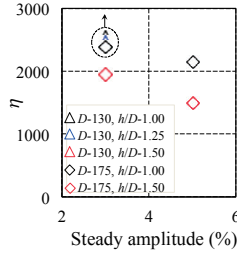


Fig. 4:  $\eta-S.a$  relation

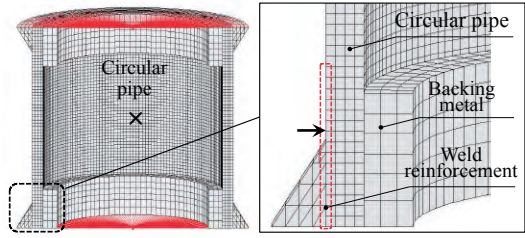


Fig. 5: Analysis modeling

exhibit stable spindle-shaped hysteresis characteristics. The failure mode is 2 type of crack at the welding toe and shear buckling. Photo 1 shows an example of failure mode for the crack. The correlation between the cumulative plastic deformation  $\eta$  at the start time of the strength degradation and the steady amplitude (hereinafter S.a) is shown in Fig. 4. In the figure, the  $\uparrow$  symbol indicates a higher deformation capacity, and there is no decrease in strength up to the final loading cycle. In the specimens under steady amplitude cyclic loading,  $\eta$  is approximately 1500 or greater, and decreases as the S.a,  $D$ , and  $h/D$  increase.

### 4. FEM analysis

An FEM analysis was carried out the experimental results of the monotonic loading test. Therefore, the FEM analysis model describes all but the upper and lower endplates, and models the circular pipe, the backing metal, and the weld reinforcements, as shown in Fig. 5. The analysis results are in good agreement with the test results. The equivalent plastic strain  $\epsilon_{eq}$  is a parameter related to ductile crack initiation. The value of  $\epsilon_{eq}$  was measured dashed lined square in right side of Fig. 5. The highest  $\epsilon_{eq}$  value was found at the weld toe ( $\rightarrow$  symbols in right side of Fig 5.), which is consistent with the position where cracking occurred, as shown in Photo 1. Figure 6 shows the relation between  $h/D$  and  $\epsilon_{eq}$  in the weld toe for  $\gamma=5\%$ ,  $10\%$ , and  $15\%$ . The value of  $\epsilon_{eq}$  for the weld toe increases with  $h/D$ , and the slope for  $D=175$  mm is considerably higher than that for  $D=130$  mm. The test results revealed that because of the presence of the backing metal, shear deformation occurred from both ends of the LYCHSD in all parts except the backing metal itself. Therefore, the effective aspect ratio is defined as  $h'/D$ , where  $h'$  is the height without the backing metal. Then, it is examined with  $\epsilon_{eq}$  that is occurred in weld toe. Figure 7 plots the relation between  $h'/D$  and  $\epsilon_{eq}$  at the weld toe at  $\gamma 5\%$ ,  $10\%$ ,  $15\%$  each.  $\epsilon_{eq}$  for the weld toe increases with  $h'/D$  increases.

### 5. Conclusion

The conclusions are listed below.

- Based on the results of a cyclic loading test, the LYCHSD exhibited stable spindle-shaped hysteresis characteristics.
- For specimens under steady-amplitude cyclic loading, the start time of the strength degradation became earlier as the diameter, aspect ratio, and amplitude increased. The cumulative plastic deformation was smaller and the deformation capacity was about 1500 or greater.
- Based on the FEM analysis results, The equivalent plastic strain at the weld toe increased with the aspect ratio, and changed rapidly as the diameter increased. In addition, the equivalent plastic strain for the weld toe had a positive correlation with the effective aspect ratio.

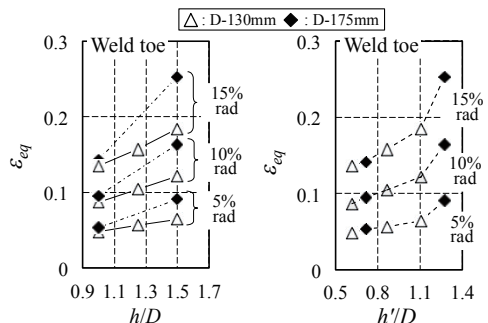


Fig. 6:  $\epsilon_{eq}-h/D$  relation Fig. 7:  $\epsilon_{eq}-h'/D$  relation